APPLICATION NOTE

A demonstration of orthogonal validation to study genes associated with metastatic phenotypes using Dharmacon™ siRNA, CRISPR knockout, and CRISPR interference reagents.

Author

Brian Ziemba
Senior Scientist, R&D, Revvity

Abstract

From RNA interference (RNAi) to CRISPR, there are several methods that researchers can use to manipulate gene function, each with its own strengths and weaknesses. Orthogonal validation—the synergistic use of different methods—makes genetic perturbation studies more robust. Utilizing complementary methods, including RNAi and CRISPR-knockout, -interference and -activation, enables researchers to have confidence in their results.

Introduction

A widely used approach for studying gene function is to reduce or disrupt its basal expression. Methods employed to knockdown or knockout gene products can answer specific questions about gene function, in addition to helping identify and develop therapeutics. RNA interference (RNAi) was the primary tool for the rapid disruption of gene expression and downstream functional characterization for many years but has recently been supplemented with newer CRISPR-based technologies, including CRISPR-knockout and CRISPR-interference (CRISPRi). Having several orthogonal technologies to disrupt a gene function, each with different mode and action, and application-specific benefits and considerations, provides an effective approach for validating findings obtained with one methodology alone.

Orthogonal validation can be used as independent assays to eliminate the possibility of false negative or positive findings. In this manner, orthogonal validation is an essential component of a well-designed and -controlled experiment. An additional benefit

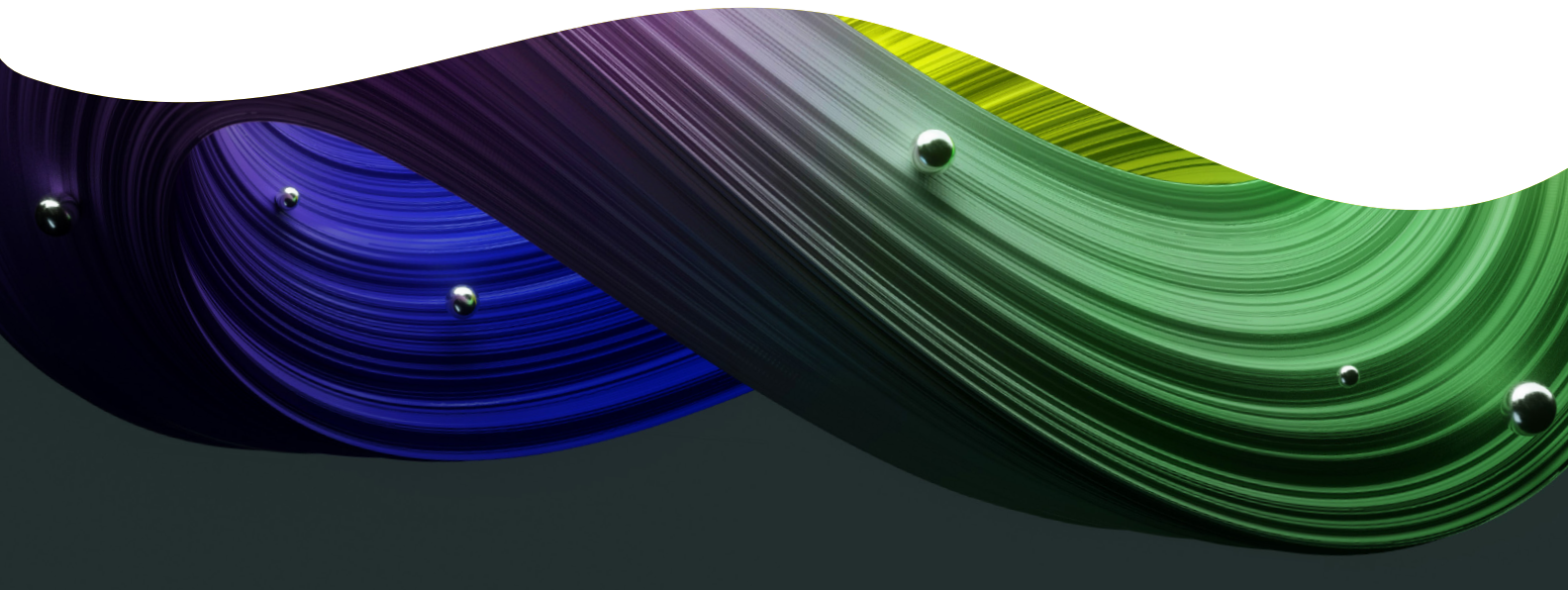

of synergistic testing is the possibility of revealing additional properties of the target gene. For example, by comparing results from RNAi and CRISPR knockout experiments, one might find that the gene product is necessary for viability, exhibits dosage effects, or is a requisite part of a cellular process. Two such studies[1,2] present an empirical rationale for pursuing a strategy based on orthogonally validating preliminary results from either of the three gene interference methods. In particular, Stojic et al found that depleting protein coding gene transcripts using different loss-of-function methods yielded method-specific off-target signatures in RNA sequencing analysis. In some cases, these transcriptomic variations led to different cellular phenotypes, and thus, different biological conclusions. These studies illustrate the risk of attributing initial findings to purported effects of the gene target under examination. In each study, the authors were able to identify data that could (likely) be traced to nonspecific effects of the experimental setup, underscoring the importance of orthogonal validation in gene interference experiments.

Here, we present an example of an orthogonal validation framework using different loss-of-function (LOF) platforms directed against specific targets involved in governing or maintaining the mesenchymal-to-epithelial transition (MET). The MET is governed by a reversible, complex, multicomponent cellular signaling network that guides the transition from motile, mesenchymal cells to nonmotile epithelial cells[3]. In this work, three target-directed LOF platforms are assessed at the level of cellular migration and adhesion markers, two phenotypic hallmarks surrounding the MET.

Evaluating MET is an attractive option to outline an orthogonal validation paradigm due to a well-characterized set of phenomena that can be measured in cell culture, such as migration and regulation of adhesion markers. Beyond the utility as a case study in orthogonal validation, MET also appears to play a central role in metastatic colonization, where mesenchymal tumor cells revert to a more epithelial state to proliferate and form growths at secondary sites[4]. Thus, LOF studies of target genes involved in regulating the invasiveness of cancer cells may be useful in designing and developing therapies to suppress metastasis, infiltration, and secondary tumorigenesis. As such, we have applied an orthogonal experimental framework utilizing target gene knockdown and knockout to four key regulators of the MET: ZEB1[5], ZEB2[6], PI3Ka[7] and AKT2[7] in a mesenchymal model for MET.

Applying the three different LOF platforms, we demonstrate the following:

- Robust target knockdown at the mRNA and protein level for four separate targets involved in MET with siRNA, CRISPR knockout or CRISPRi LOF platforms.
- All three LOF methods demonstrated exhibited decreased cell migration when targets involved in maintaining mesenchymal phenotype were targeted.
- LOF studies targeting the same four targets exhibited some differences in expression of cellular adhesion markers involved in governing the transition between mesenchymal and epithelial phenotypes.

Results

Stable cell generation, target gene knockdown/knockout, and analysis

To apply similar methods and assay formats, we used synthetic RNAs for each technology (siRNA for RNAi and synthetic gRNAs for CRISPR knockout and CRISPR interference) and cells that stably express relevant Cas9 effectors. To generate cells that stably express WT Cas9 (KO-competent) and dCas9-SALL1-SDS3[8] (CRISPRi-competent), relevant lentiviral particles were transduced into mesenchymal cells and expanded under selection. Transfection with appropriate sgRNA controls revealed appropriate control gene target knockdown or knockout (data not shown).

Next, mesenchymal cells were transfected with siRNA directed against non-targeting control sequences (NTC) along with siRNA specific for MET targets ZEB1, ZEB2, PI3Ka and AKT2. In parallel, KO- or CRISPRi-specific sgRNA for the same targets were transfected into mesenchymal cells that were stably expressing WT Cas9 or dCas9-SALL1-SDS3, respectively. T7E1 and RT-qPCR analysis of subsequent cell lysates reveal effective knockout (35-40% indels at target gene in experimental cell populations), or knockdown (85-90% target gene knockdown with siRNAs and 50-85% knockdown with CRISPRi) in all three LOF platforms and MET targets under study (Fig 1).

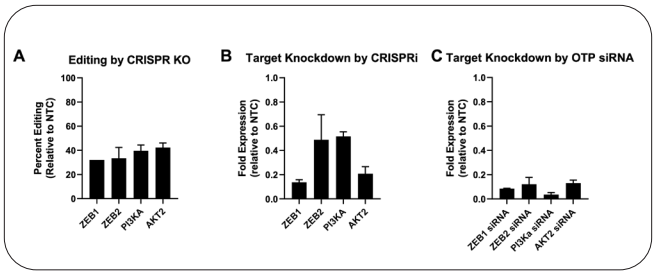

Figure 1: Target gene editing and knockdown assessment from loss-of-function experiments. T7E1 after target gene knockout (A), and qPCR analysis of target knockdown after CRISPRi (B) and siRNA (C) were assessed 72 hours post reagent transfection. Data derived from triplicate experiments on two separate days.

To fully characterize the efficacy of gene knockout or knockdown at the protein level, resulting target protein abundance was assessed with Western Blotting (WB). WB results from all three LOF technologies were in-line with genetic analyses, revealing 50-80% target protein depletion at the 72-hour timepoint Figure 2).

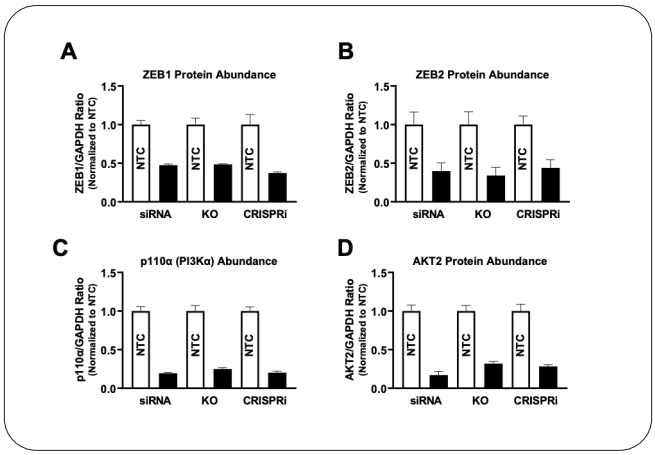

Figure 2. Assessment of target protein abundance after target gene loss-of-function experiments. Western Blotting analysis of ZEB1 (A), ZEB2 (B), PI3Kα (C) and AKT2 (D) protein levels 72 hours after initiation of loss-of-function experiments.

Target MET gene attenuation by siRNA, CRISPR knockout or CRISPR interference results in loss of cellular mobility

To determine whether target MET gene knockout or knockdown using the three LOF methods affect cell migration, a second-generation cell migration assay was employed. The assay, which involves culturing cells around a removable stopper, then tracking cell migration into the detection zone after stopper removal, overcomes limitations of the traditional scratch assay such as subjective analysis, and difficulties with reproducibility. Example images of this occlusion zone assay (Fig3A) demonstrate slower mesenchymal cell migration into the central cell-free zone

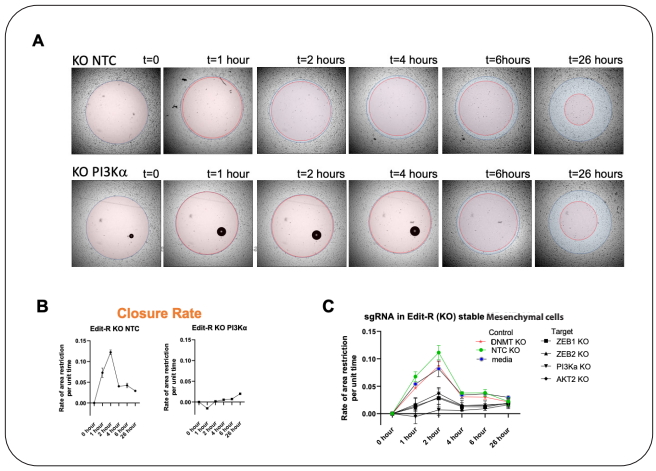

Figure 3: Migration Analysis Workflow. Raw images of Cas9 stable cells transfected with NTC or PI3Kα-targeting sgRNA from migration assay (A). Images overlaid with blue mask to indicate starting position of cell boundary and red mask to track cell boundary at designated time period. Migration capacity assessed by determining the difference in area per unit time, generating a closure rate trace (B). Closure rate traces from KO, siRNA and CRISPRi target and control experiments were combined to compare phenotypic outcomes (C).

when target MET gene PI3Ka knockout is compared relative to an NTC control sgRNA. Closure rate was periodically tracked over the course of 26 hours after experiment initiation, and bulk cell migration speed at individual timepoints were extracted to assemble migration speed traces (Fig 3B). Fig 3C presents migration speed traces for controls and MET target CRISPR knockout experiments. Notably, in parallel experiments, siRNA, CRISPR knockout and CRISPRi migration traces exhibit the same trend of migration speed differentials peaking between 1-2 hours, then matching control speed by experimental termination.

Comparisons of migration speed between LOF methods and different MET targets can be made by calculating the area under the curve (AUC) of closure rate traces presented in Fig 3B. Figure 4A, B and C present AUC comparisons of the three LOF platforms with relevant controls and MET gene targets, highlighting statistically significant decreases in migration capacity for the four experimental target genes.

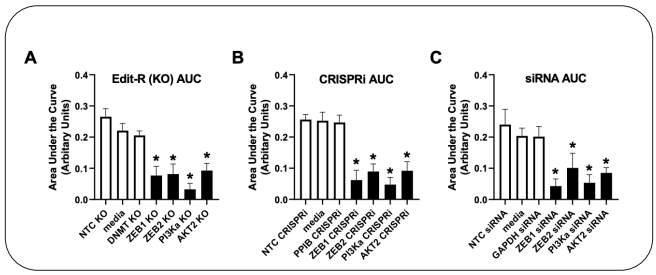

Figure 4: Area Under the Curve (AUC) Analysis of Cell Migration from LOF Experiments. AUC calculations from migration closure rate traces for KO (A), CRISPRi (B) and siRNA (C) LOF experiments. Asterisks indicate significance of each experimental result as compared to the change of NTC control cell migration at $p < 0.05$.

Adhesion marker perturbations associated with MET gene targets are associated with some, but not all LOF methods

Fluorescent immunocytochemistry was used to evaluate levels of expressed E-cadherin and vimentin after target MET genes were attenuated by either siRNA, CRISPR knockout or CRISPRi in mesenchymal cells (Fig 5A, B, C). The transition from mesenchymal to epithelial cells coincides with a gradual increase in levels of E-cadherin and decrease in vimentin, resulting in an increase in the ratio of E-cadherin:vimentin. LOF experiments yielded cells exhibiting significantly increased E-cadherin:vimentin ratios in siRNA and CRISPR knockout experiments for all 4 target genes, and ratios that trended upwards for two of the target genes only (ZEB1 and ZEB2) in CRISPRi experiments (Fig 4D).

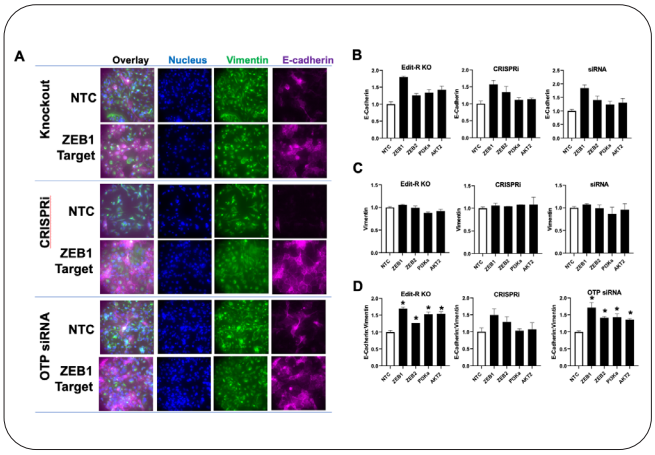

Figure 5. Cadherin:Vimentin Ratio Perturbation in LOF Experiments. Example of immunofluorescent imaging after ZEB1 knockdown / knockout or control experiments (A) displaying nuclear, Vimentin and E-cadherin on separate imaging channels. Integration of E-cadherin (B) and vimentin (C) signals indicating target prevalence. Ratio of E-cadherin to vimentin (D) results in LOF experiments. Asterisks indicate significance of each experimental result as compared to the change of NTC control ratio at $p < 0.05$.

Discussion

With any experiment, inclusion of proper controls ensures the validity of results. An important addition to a composite of controls is orthogonal validation, which ensures that methodologic artifacts are not influencing experimental outcomes. To present an orthogonal validation framework, we employed the Dharmacon Reagents' gene loss-of-function platforms to eliminate, or lower, the abundance of specific cellular targets that either control or influence measurable mesenchymal cell phenotypes. To this end, OTP siRNA was applied to mesenchymal cells while pre-designed Edit-R™ KO or CRISPRi-specific sgRNA was transfected into mesenchymal cells stably expressing WT Cas9 or Cas9-SALL1-SDS3, respectively.

Effectiveness of LOF technology was gauged with T7E1, qPCR and Western Blotting and compared with phenotypic landmarks that characterize mesenchymal cell nature, beginning with cellular migration. In this study, we determined that siRNA, CRISPR KO and CRISPRi were all equally efficacious at transitioning mesenchymal cells toward a more epithelial nature, as indicated by significantly slower cell migration. Using all three LOF platforms in parallel, a productive knockout or knockdown MET gene targets significantly slowed cellular migration, and there were no significant differences in migration effect between LOF platform within each target.

Cellular adhesion markers, which are another functional and phenotypic marker of mesenchymal and epithelial cells, were also assessed. In contrast to the observed migration phenotype, increases in E-cadherin to vimentin ratio (E-cad:Vim) were not always correlated with all three LOF platforms. While target knockout with standard CRISPR Cas9 and knockdown by siRNA were correlated with significant increases in the E-cad:Vim), target knockdown by CRISPRi provoked a more blunted response in two of the four gene targets (PI3Ka and AKT2).

The differential effects on E-cad:Vim between the three LOF platforms is likely due to differences in timing, kinetics or completeness of loss of target function. Since Western blotting data indicates that CRISPRi is similarly efficacious at depleting target MET proteins when compared to parallel experiments with CRISPR knockout and siRNA, it is possible that nuances in cellular kinetics or target depletion trajectories may affect endpoint measurements for some outcomes.

Gene interference is, due to the invasive properties of the method (forcing reactive nucleases and or RNA into cells), a complicated, but powerful experiment, with many factors involved, including experimental hypotheses, gene targets and cell type under study. Diverse phenotypic readouts, due to systemic complexities and variable kinetics can be differentially affected by choice of LOF platform. However, when properly controlled and validated, resultant experimental data can be of high quality and reproducible.

In this study, we have highlighted the use of different loss-of-function technologies to complicated cellular assays to study cellular migration and the MET. These findings underscore the importance of orthogonal validation in experiments involving complex phenotypes and outcomes. In many cases, orthogonal, or independent, validation is a requisite addition to the gene editing toolbox and can ensure that consequent findings are arrived at in the most reliable and efficient manner, and that the correct gene-function relationships are uncovered.

Materials and Methods

Stable Cell Generation

Mesenchymal cell lines that stably express Cas9 nuclease or dCas9-SALL1-SDS3, were generated using lentiviral particles containing either a codon-optimized version of the Cas9 gene (Horizon Discovery™, VCAS10126) or the dCas9-SALL1-SDS3 construct (Horizon Discovery™, VCAS12247), respectively. Cells were seeded in 24-well plates and grown to 80-90% confluency, then transduced with lentiviral particles according to a multiplicity of infection (MOI) from 0.1 to 0.4. Cultures were grown under blasticidin selection (13 µg/mL, optimized for current cell line, data not shown) for 72 hours, then split into 6-well plates. Cells transduced under 0.1 MOI were deemed optimal due to growth parameters under selection and were expanded twice more until seeding was possible in T75 flask. Control experiments confirmed that generated cell lines were able to attenuate expression of test genes (data not shown) and deemed appropriate for further experimentation.

Tissue Culture

Mesenchymal cells, stable Cas9 and stable dCas9-SALL1-SDS3 mesenchymal cell lines were maintained in established media (high glucose DMEM with 10% (v/v) FBS and 2 mM L-glutamine) at 37°C and 5% CO_2. Cells were passaged by rinsing with calcium-free PBS, incubating with 0.25% trypsin for 5 minutes at 37°C, then diluting with full media and reseeding on fresh 96-well plates.

Transfections

For siRNA and sgRNA transfections, wild-type and stable mesenchymal cells were seeded in 96-well plates at 5K cells / well. After 24 hours of growth at 37°C and 5% CO_2, transfections were carried out by replacing cell media with suspensions of 44 nM siRNA and 0.2 µL DharmaFECT 1 per well in wild-type mesenchymal cells or 22 nM sgRNA and 0.2 µL DharmaFECT 4 per well in stable cell lines. Cultures were unperturbed for 72 hours prior to endpoint experiments.

RT-qPCR and T7E1 Analysis

RT-qPCR was used to assess RNA levels for relative target and control genes in knockdown experiments at 72 hours post-transfection. Total RNA was isolated from cell lysates using an SV 96 Total RNA Isolation System (Promega, Z3500). From RNA isolates, cDNA was synthesized using a Maxima First Strand cDNA Synthesis Kit (Thermo, K1672). 7.5 uL TaqMan Master Mix (Thermo, 4304437) was mixed with 2.0 uL undiluted cDNA and 0.5 uL of appropriate TaqMan probe (Thermo, beta-actin, Hs03023943_g1; ZEB1, Hs01566408_m1; ZEB2, Hs00207691_m1, AKT2, Hs01086099_m1; PIK3CA [PI3Ka], Hs00907957_m1). Samples were mixed and 10 uL of each reaction was transferred to individual wells on a 384-well plate and loaded onto a Roche LightCycler 480 II for thermal cycling and analysis. Each sample was performed in technical duplicate. The relative expression of each target gene was calculated with the ΔΔCq method using beta-actin as the housekeeping gene and normalized to a non-targeting control.

T7E1 assay was used to determine efficacy of gene knockout experiments for target and controls genes at 72 hours post-tranfection. For this analysis, cellular DNA was isolated by lysing cultures in a mixture of proteinase K and RNAse A at 56°C, followed by enzyme inactivation at 96°C. Amplicons spanning the edit window were amplified from genomic DNA in resultant lysate using touchdown PCR and predesigned detection primers (Horizon). PCR product was heated to 95°C for 10 minutes and cooled to 25°C over 20 minutes, then incubated with T7 endonuclease and analyzed on an agarose gel. Full protocol can be found here.

Western Blotting

For analysis of protein expression after knockdown and knockdown experiments, cell transfections were scaled up to 6-well plates. Mesenchymal wild-type and stable cells were plated at 300k cells / well and all other reagents were scaled accordingly. After 72 hours post-transfection, cells were scraped in lysis buffer (150mM NaCl, 50mM TRIS pH 7.4, 1mM EDTA, 1X TritonX-100 and 0.01X HALT protease and phosphatase inhibitor cocktail (Thermo, 78440)). After a 10 min incubation on ice, lysates were spun at 12k RPM

at 4°C, and supernatants were retained. Lysate protein content was assessed via BCA assay and 12 mg total protein per sample was electrophoresed on a 4-12% Bis-Tris NuPAGE protein gel (Thermo, NPO336BOX) at 180V for 1 hour. Protein was transferred to 0.2mm nitrocellulose membrane using an XCell II Blot Module (Thermo) at 200mA for 2 hours in transfer buffer with 5% methanol. Membranes were washed twice in 1X PBS-T for 3 minutes, then added to 20 mL blocking buffer (Thermo; Superblock T20, 37516). Membranes were cut near 45 kDa marker standard to separate loading control (GAPDH ~ 37 kDa) and targets of higher molecular weight (ZEB1 at 124 kDa, ZEB2 at 136 kDa, AKT2 at 56 kDa and PI3K p110a at 110 kDa. Membranes were incubated with GAPDH antibody (Biolegend, 649202) at 1:10,000 dilution while ZEB1 (CST, D80D3), ZEB2 (CST, E6U7Z), AKT2 (CST, D6G4) and PI3K p110a (CST, C73F8) antibodies were added to blocking buffer at 1:1000 dilution. Membranes were incubated with primary antibodies overnight at 4°C with rocking, then washed four times in 1X PBS-T for 3 minutes. Secondary anti-rabbit HRP-conjugated antibody (Invitrogen, A16096) was incubated with ZEB1-, ZEB2-, AKT2-, and PI3K p110a-probed membrane at 1:10,000 dilution while anti-mouse HRP-conjugated antibody (Pierce, 31431) was incubated with GAPDH-probed membrane at 1:10,000 dilution. Membranes were rocked with secondary antibody dilutions for 2 hours at room temperature. Membranes were again washed four times in 1X PBS-T for 3 minutes and incubated with chemiluminescent substrate for 15 seconds before imaging (Invitrogen, iBright 1500 FL).

Migration Analysis

Cell migration was evaluated with Oris Cell Migration Assay plates (Platypus Technologies, CMACC1.101). Briefly, plates coated with collagen I were seeded with 5K wild-type and stable mesenchymal cells / well, then transfected after 24 hours under conditions described above. At 72 hours post-transfection, occlusion stoppers were removed with included removal tool. Pre-migration zone (zone of absent cell growth) shape and size was immediately measured in all conditions using a Nikon Eclipse Ti in brightfield mode at 10X magnification. Plate was incubated at 37°C and 5% CO_2 for duration of experiment, and re-imaged periodically over 26 hours. Resultant images were analyzed using ImageJ manually and with the MRI Wound Healing Tool macro[9, 10].

Immunocytochemistry (ICC)

For immunocytochemical analysis, cells were processed on the 96-well glass culture support. After removing media, 4% paraformaldehyde (PFA) fixative was added for 30 minutes at room temperature, then washed twice with PBS. Cells were permeabilized by incubating with 0.5% (v/v) Triton X-100 in PBS for 15 minutes at room temperature and washed three times with PBS. After blocking cells with 3% (w/v) BSA in PBS for 30 minutes at room temperature, 1:500 rabbit-derived anti-E cadherin (Abcam ab40772) and 1 ug/mL mouse-derived anti-vimentin (Abcam, ab8978) were added to blocking solution for a 1 hour incubation at room temperature with gentle rotation. Cells were then washed three times with PBS with 0.1% (w/v) BSA and 0.1% (v/v) Triton X-100, then incubated with fluorescent secondary detection antibodies (1:1000 dilutions of each goat anti-rabbit conjugated to AF488 [Thermo, A32731] and donkey anti-mouse conjugated to AF647 [Thermo, A31571]) in PBS. After three washes with PBS with 0.1% (w/v) BSA and 0.1% (v/v) Triton X-100, 1 ug/mL Hoeschst 33342 in PBS was added for 15 minutes at room temperature followed by three washes in PBS. Wells were left in 100 uL PBS and sealed for imaging. Fluorescent images were captured at 20X magnification using a Nikon Eclipse Ti and processed with CellProfiler image analysis software and Prism (GraphPad).

References

1. Smith I, Greenside PG, Natoli T, Lahr DL, Wadden D, Tirosh I, Narayan R, Root DE, Golub TR, Subramanian A, Doench JG. Evaluation of RNAi and CRISPR technologies by large-scale gene expression profiling in the Connectivity Map. PLoS Biol. 2017 Nov 30;15(11):e2003213. doi: 10.1371/journal.pbio.2003213. PMID: 29190685; PMCID: PMC5726721.

2. Stojic L, Lun ATL, Mangei J, Mascalchi P, Quarantotti V, Barr AR, Bakal C, Marioni JC, Gergely F, Odom DT. Specificity of RNAi, LNA and CRISPRi as loss-of-function methods in transcriptional analysis. Nucleic Acids Res. 2018 Jul 6;46(12):5950-5966. doi: 10.1093/nar/gky437. PMID: 29860520; PMCID: PMC6093183.

3. Sipos F, Galamb O. Epithelial-to-mesenchymal and mesenchymal-to-epithelial transitions in the colon. World J Gastroenterol. 2012 Feb 21;18(7):601-8. doi: 10.3748/wjg.v18.i7.601. PMID: 22363130; PMCID: PMC3281216.

4. Yang J, Antin P, Berx G, Blanpain C, Brabletz T, Bronner M, Campbell K, Cano A, Casanova J, Christofori G, Dedhar S, Derynck R, Ford HL, Fuxe J, García de Herreros A, Goodall GJ, Hadjantonakis AK, Huang RYJ, Kalcheim C, Kalluri R, Kang Y, Khew-Goodall Y, Levine H, Liu J, Longmore GD, Mani SA, Massagué J, Mayor R, McClay D, Mostov KE, Newgreen DF, Nieto MA, Puisieux A, Runyan R, Savagner P, Stanger B, Stemmler MP, Takahashi Y, Takeichi M, Theveneau E, Thiery JP, Thompson EW, Weinberg RA, Williams ED, Xing J, Zhou BP, Sheng G; EMT International Association (TEMTIA). Guidelines and definitions for research on epithelial-mesenchymal transition. Nat Rev Mol Cell Biol. 2020 Jun;21(6):341-352. doi: 10.1038/s41580-020-0237-9. Epub 2020 Apr 16. Erratum in: Nat Rev Mol Cell Biol. 2021 Dec;22(12):834. PMID: 32300252; PMCID: PMC7250738.

5. Zhang P, Sun Y, Ma L. ZEB1: at the crossroads of epithelial-mesenchymal transition, metastasis and therapy resistance. Cell Cycle. 2015;14(4):481-7. doi: 10.1080/15384101.2015.1006048. PMID: 25607528; PMCID: PMC4614883.

6. Qi S, Song Y, Peng Y, Wang H, Long H, Yu X, Li Z, Fang L, Wu A, Luo W, Zhen Y, Zhou Y, Chen Y, Mai C, Liu Z, Fang W. ZEB2 mediates multiple pathways regulating cell proliferation, migration, invasion, and apoptosis in glioma. PLoS One. 2012;7(6):e38842. doi: 10.1371/journal.pone.0038842. Epub 2012 Jun 26. PMID: 22761708; PMCID: PMC3383704.

7. Xu W, Yang Z, Lu N. A new role for the PI3K/Akt signaling pathway in the epithelial-mesenchymal transition. Cell Adh Migr. 2015;9(4):317-24. doi: 10.1080/19336918.2015.1016686. Epub 2015 Aug 4. PMID: 26241004; PMCID: PMC4594353.

8. Welcome to the toolbox, CRISPRi. (horizondiscovery.com)

9. Cormier N, Yeo A, Fiorentino E, Paxson J. Optimization of the Wound Scratch Assay to Detect Changes in Murine Mesenchymal Stromal Cell Migration After Damage by Soluble Cigarette Smoke Extract. J Vis Exp. 2015 Dec 3;(106):e53414. doi: 10.3791/53414. PMID: 26709527; PMCID: PMC4692776.

10. Jonkman JE, Cathcart JA, Xu F, Bartolini ME, Amon JE, Stevens KM, Colarusso P. An introduction to the wound healing assay using live-cell microscopy. Cell Adh Migr. 2014;8(5):440-51. doi: 10.4161/cam.36224. PMID: 25482647; PMCID: PMC5154238.

Revvity
940 Winter Street
Waltham, MA 02451 USA

(800) 762-4000
www.revvity.com

For a complete listing of our global offices, visit www.revvity.com